

# The role of wetlands in the chromophoric dissolved organic matter release and its relation to aquatic ecosystems optical properties. A case of study: Katonga and Bunjako Bays (Victoria Lake; Uganda)

Luca Bracchini <sup>a,b,\*</sup>, Andrés Cózar <sup>a,c</sup>, Arduino Massimo Dattilo <sup>a,b</sup>,  
Steven Arthur Loiselle <sup>a,b</sup>, Antonio Tognazzi <sup>a,b</sup>, Nicolas Azza <sup>d</sup>,  
Claudio Rossi <sup>a,b</sup>

<sup>a</sup> *Department of Chemical and Biosystem Sciences and Technologies, Siena University, Via A. Moro 2, 53100 Siena, Italy*

<sup>b</sup> *Consorzio interuniversitario per lo sviluppo dei Sistemi a Grande Interfase, CSGI—Via della Lastruccia 3-50010 Sesto Fiorentino, Florence, Italy*

<sup>c</sup> *Area de Ecología, Facultad de Ciencias del Mar, University of Cadiz, 11150 Cádiz, Spain*

<sup>d</sup> *Directorate of Water Development, P.O. Box 19, Entebbe, Uganda*

Received 9 March 2005; received in revised form 1 September 2005; accepted 7 September 2005

Available online 10 November 2005

## Abstract

Chromophoric Dissolved Organic Matter (CDOM) is an important component in freshwater and marine ecosystems and plays direct and indirect role in biogeochemical cycles. CDOM originates from the degradation process of organic materials, usually macrophytes and planktons. The present work examines the importance of wetland derived CDOM on the optical and bio-optical properties of two bays of Lake Victoria (Uganda, Africa). This was achieved by determining the attenuation and extinction coefficients of filtered and unfiltered water samples from two equatorial bays on the Ugandan coastline of Lake Victoria. Katonga Bay is a wetland lined bay that receives water from the Katonga river, while Bunjako Bay is an outer bay between Katonga Bay and Lake Victoria. The results showed that attenuation was highest in Katonga Bay and the role of CDOM is most dominant near the river inlet. The quantity and quality of CDOM is extremely different in the two bays: in Katonga Bay it is possible to hypothesize a terrestrial origin of CDOM (transported by the wetland river). On the contrary, in Bunjako Bay, spectral measurements of absorption indicate a modified CDOM and/or alternative CDOM source. The terrestrial CDOM in Katonga Bay is more capable of absorbing harmful UV radiation than the CDOM present in the Bunjako Bay. The resulting optical environment in the former bay presented a water column with a very limited penetration of harmful UV radiation, while a higher penetration was observed in the Bunjako Bay. © 2005 Elsevier Ltd. All rights reserved.

*Keywords:* Wetland; CDOM; UV; Statistical modeling

\* Corresponding author. Address: Department of Chemical and Biosystem Sciences and Technologies, Siena University, Via A. Moro 2, 53100 Siena, Italy. Tel.: +39 0577 234369; fax: +39 0577 234177.

E-mail address: [bracchini@unisi.it](mailto:bracchini@unisi.it) (L. Bracchini).

## 1. Introduction

Dissolved Organic Matter (DOM) in aquatic ecosystems is a mixture of molecules with molecular weight between 500 and  $1 \times 10^6$  Da. DOM is largely composed by aromatic and aliphatic polymer-like compounds and while it is impossible to give it a structural chemical definition, an operative definition has been given: DOM is the dissolved organic matter not retained in the filtration of water samples. Several authors use 0.45  $\mu\text{m}$  filter units to separate DOM or dissolved organic carbon from suspended substances (e.g. Kalbitz et al., 2000; McDonald et al., 2004; Akkanen et al., 2005), while others use 0.22  $\mu\text{m}$  filters (e.g. De Haan, 1972; Peuravuori and Pihlaja, 1997; Huovinen et al., 2003). The comparison between results obtained with different filters (type and nominal pore size) is difficult and a standardization of adopted methods has been recommended (Danielson, 1982).

Chromophoric Dissolved Organic Matter (CDOM) is defined as the optically active fraction of DOM. Within the water column, CDOM is a major bio-optical constituent in the attenuation of the solar ultraviolet radiation (UV, 290–400 nm) (Morris et al., 1995; Shindler et al., 1996). Visible radiation (400–700 nm) is also influenced by CDOM, in particular at lower wavelengths (400–500 nm) (Markager and Vincent, 2000; Bracchini et al., 2004a; Zanardi-Lamardo et al., 2004).

The main sources of DOM in aquatic ecosystems are the degradation of terrestrial plant matter and the in situ production related to the degradation of aquatic macrophytes and phytoplankton (Kirk, 1994; McKnight and Aiken, 1998). DOM plays a crucial role in the biogeochemical cycles of the aquatic ecosystems (Williamson et al., 1999; Hunt et al., 2000; Hansell and Carlson, 2002), and its functionality is influenced by climate change and ozone depletion (Zepp et al., 2003). The degradation of DOM by biological activity or solar irradiance fluxes (e.g. ultraviolet radiation) can influence bacterial activity and phytoplankton growth by increasing the availability of degraded (more edible) fraction of DOM (Corin et al., 1998; Zafriou, 2002).

The photodegradation of CDOM is the process in which CDOM is broken down into smaller compounds following the absorption of photons in the UV and visible wavelengths. This degradation may lead to a reduction in the absorption of incoming solar radiation (photobleaching) and formation of toxic photoproducts (e.g. singlet oxygen production; Haag et al., 1984; Backlund, 1992; Corin et al., 1996; Grzybowski, 2000; Osburn and Morris, 2003; Zepp, 2003).

Photobleaching of CDOM will increase the penetration of UV and visible radiation in the water column, with important consequences on the biotic community (Vincent et al., 1998). The present work focuses on the role that wetlands play in the release of chromophoric

dissolved organic matter, using in situ and laboratory spectroscopic approaches. Furthermore, we examine the importance of CDOM in conditioning the aquatic ecosystems optical properties.

## 2. Materials and methods

### 2.1. Study site

Katonga and Bunjako Bays are located in the Ugandan section of Lake Victoria. These bays are located at an equatorial latitude at 32° East. The former (Fig. 1a) is surrounded by papyrus dominated littoral wetlands on three sides and has a surface area of 10 km<sup>2</sup>. Katonga Bay receives inflow from the Katonga river in its north-western corner. Bunjako Bay (30 km<sup>2</sup>) is located between Katonga Bay and the open Lake Victoria area. This bay has a lower percentage of coastal wetland (15%).

### 2.2. Optical and bio-optical measurements

Measurements were conducted at 46 stations between 10:30 and 14:30 local hour over two days (25–26 October, 2002; Fig. 1b) in low wind condition and substantial clear sky. Transects were executed in western–eastern and eastern–western directions, visiting stations of Katonga and Bunjako Bays each day.

In each station, a vertical profile of the UV and Photosynthetic Active Radiation (PAR) irradiances were measured using a PUV541 spectroradiometer SN 19235 (Biospherical Instruments, San Diego, CA). The PUV541 measures irradiance at four UV wavelengths: 305 nm (bandpass 7 nm), 313 nm (bandpass 10 nm), 320 nm (bandpass 11 nm) and 340 nm (bandpass 10 nm) with a cosine response. The instrument was calibrated in July 2001. Absolute calibration (using a NIST-traceable 1000 W FEL-type standard spectral irradiance lamp) and relative calibration were executed, by comparing the measured solar irradiances with a second spectroradiometer (SUV-100, Biospherical Instruments) with a spectral resolution of 1 nm. After relative calibration, the PUV541 is able to measure spectral irradiance ( $\mu\text{W cm}^2 \text{nm}^{-1}$ ) comparable with SUV-100 spectroradiometer.

The instrument was manually lowered from the sun illuminated side of the boat. To reduce the interferences, a 2.00 m extension was used to increase the distance between the instrument and the boat. At the end of the extension, a pulley was used to facilitate the downward and upward casting of the instrument. At each station, irradiance measurements were acquired simultaneously every 0.3 s. Depth ( $\pm 2$  cm) was measured simultaneously to create an irradiance profile along the water column. Depth was measured using a pressure sensor, calibrated to 2 cm for measurements just below the

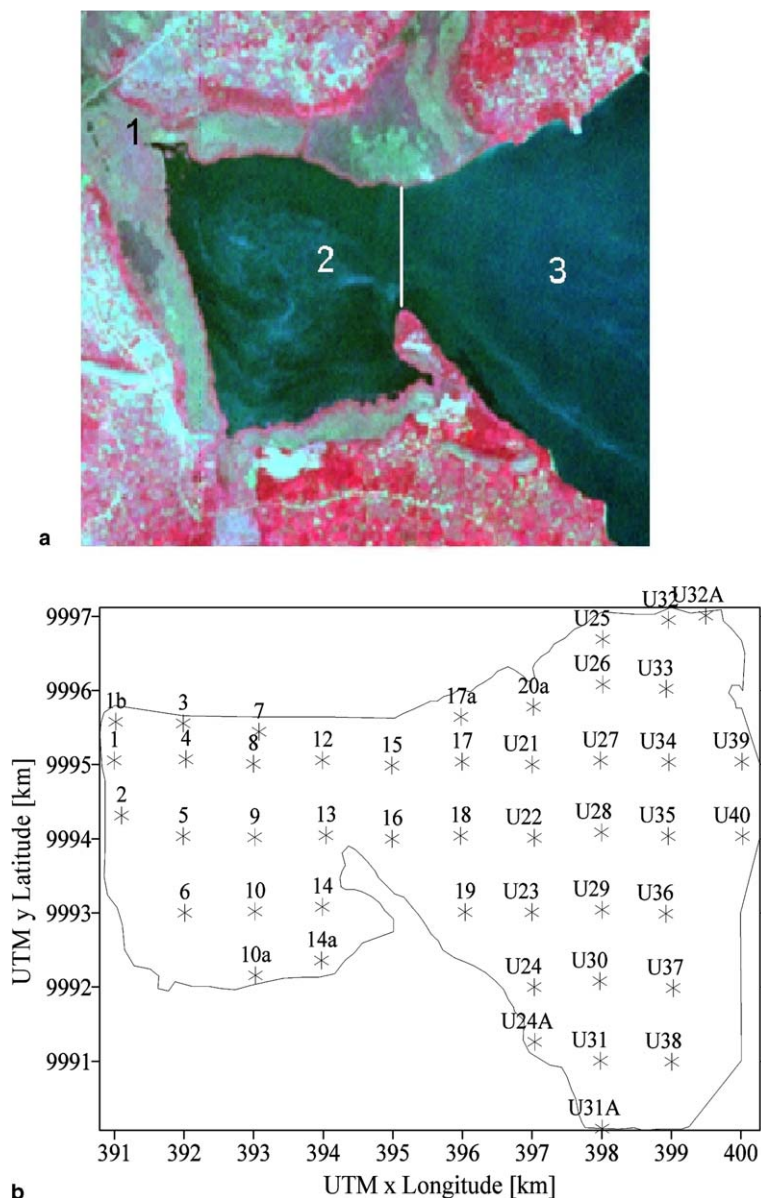


Fig. 1. (a) Satellite image of the study site (Landsat ETM). The Katonga river (1) is shown together with Katonga Bay (2) and Bunjako Bay (3). The line is an approximate separation of the two bays. (b) Map representation of the sampling stations in Katonga and Bunjako Bays.

water surface, to allow for changes in atmospheric pressure. A dark file of PUV measurements (about 1000 record) were recorded at each station to check the stability of the irradiance and depth measurements. The irradiance measurements were initiated below the surface water line (about 2 cm) and were recorded while the instrument was lowered to just about the lake bottom as well as during the raising of the instrument. On average, 100 measurements (irradiance and water depth (m)) were obtained in each profile. The resulting radia-

tion profile was corrected by removing the dark current signal ( $<0.001 \mu\text{W cm}^{-2} \text{nm}^{-1}$ ) and plotted against the water depth. The diffuse attenuation coefficient was calculated by fitting the best exponential curve to the profile data for each wavelength following:

$$I_{\lambda} = I_{0,\lambda} \exp(-K_{d,\lambda}(z - z_0)) \quad (1)$$

In Eq. (1)  $z$  is water depth,  $z_0$  is 2 cm,  $I_{0,\lambda}$  is the irradiance at 2 cm and  $K_{d,\lambda}$  is the spectral diffuse attenuation coefficient for the downward solar radiation at  $\lambda$ . An

analogous procedure was used for the PAR irradiance ( $\mu\text{Einstein m}^{-2} \text{s}^{-1}$ ; 1 Einstein = 1 mole of photons =  $6.022 \times 10^{23}$  photons) measurements substituting the wavelength  $\lambda$  with  $\Delta\lambda = \text{par}$ . A non linear curve fitting approach was used to fit the exponential decline in irradiance with depth. Estimations of  $K_{d,\lambda}$  were accepted when correlation coefficients were above 0.80. The best spectral fitting was found using the Levenberg–Marquardt Algorithm (LMA) least square method (using Origin 6.0 software) which can be optimized for a non linear curve fitting.

Water samples were collected at a depth of 0.2 m and filtered in situ with a 0.22  $\mu\text{m}$  single use filter (Millex GP Filter Unit, Millipore S.A., Malsheim, France), according to Grzybowski (2000). A second unfiltered sample was also collected at the same depth. Filtered and unfiltered samples were preserved in the dark at 4 °C until the spectrophotometric analysis (24 h after sampling).

The extinctions of the filtered samples were measured between 270 nm and 400 nm using a Varian Cary 50 spectrophotometer (speed scan of 4500  $\text{nm min}^{-1}$ ; monochromator type). A single quartz cuvette of 1 cm of path length and a blank of Milli-Q water were used. After acclimation in a temperature controlled room (18 °C), three different scans were performed for each sample and average values were computed for all samples where the differences between scans was less than  $10^{-3}$ . The extinction was measured with spectral resolution of 1 nm. The extinction curves were analyzed according to Bricaud et al. (1981) with the introduction of a background parameter ( $\gamma$ ,  $\text{cm}^{-1}$ ) according to the Eq. (2) (Markager and Vincent, 2000; Stedmon et al., 2000; Bracchini et al., 2004b):

$$a(\lambda) = \theta e^{s(\lambda_0 - \lambda)} + \lambda \quad \text{with } 270 \text{ nm} \leq \lambda \leq 400 \text{ nm} \quad (2)$$

where  $\lambda_0$  is 290 nm,  $\theta + \lambda$  is the absorbance at 290 nm with  $\gamma$  additional background parameter and  $s$  ( $\text{nm}^{-1}$ ) is the spectral slope of the spectra ( $s$ ,  $\theta$  and  $\gamma$  were estimated using LMA method). Slopes are presented where correlation coefficients between the estimated extinction curve and the measured absorbance were greater than 0.998. It is possible to better understand the difference between the spectral properties of CDOM (and its origin) in the two bays by representing the spectral slope vs. the absorption coefficient at 313 nm ( $A_{f,313}$ ,  $\text{m}^{-1}$ ; according to a modified approach proposed by Stedmon and Markager (2001, 2003)) of the filtered water sample.

The extinction coefficients of the unfiltered samples were determined with the same procedure but only for 305, 313, 320 and 340 nm wavelengths, to reduce the time necessary for the measurement and limiting the settlement of the suspended particles in the quartz cuvette. In the unfiltered sample, the signal recorded by the spectrophotometer (a collimated instrument) is dominated by scattering of suspended particles (and their absorp-

tion) and by the direct absorption of CDOM (after subtracting the Milli-Q water extinction; Bracchini et al., 2005a).

The ratio of extinctions of the dissolved fraction with respect to the total extinction is ( $P_{f,\lambda}$ , dimensionless) defined as

$$P_{f,\lambda} = \left[ \frac{a_f}{e_{nf}} \right]_{\lambda} = \left[ \frac{e_{nf} - e_{nf} + a_f}{e_{nf}} \right]_{\lambda} = \left[ 1 - \frac{e_{nf} - a_f}{e_{nf}} \right]_{\lambda} = 1 - P_{nf-f,\lambda} \quad (3)$$

where  $e_{nf}$  is the extinction measurement of unfiltered sample and  $a_f$  is the extinction measurement of the filtered sample. Likewise,  $P_{nf-f,\lambda}$  represents the percentage of the extinction, in the spectrophotometer, caused by suspended particles (with dimension greater than  $>0.22 \mu\text{m}$ ).  $K_{d,\lambda}$  is classified as an Apparent Optical Properties (AOPs) because its value can change with variations of quality of incident light (e.g. solar zenith angle). The measured  $a_{\lambda,f}$  is classified as Inherent Optical Properties (IOPs) because it characterizes the optical quality of the water column, regardless of the incident light. In the solar UV spectral band,  $K_{d,\lambda}$  is considered as a “quasi inherent optical property” (Baker and Smith, 1979; Zheng et al., 2002) because of its weak dependence on the solar zenith angle. In many cases, a linear relation between  $K_{d,\lambda}$  and  $a_{\lambda,f}$  ( $K_{d,\lambda} = m \times a_{\lambda,f} + b_{\lambda}$ ) is found. When a 1 cm path length cuvette is used, the angular coefficient ( $m$ ) ranges from 200 to 300  $\text{m}^{-1}$  (typically close to 230  $\text{m}^{-1}$ ; Bracchini et al., 2005b). It should be noted that  $a_{\lambda,f}$  corresponds to a monochromatic extinction measurement and  $K_{d,\lambda}$  covers a narrow extinction band which is sensitive to changes in spectral shift. However, using sensors with a 10 nm bandwidth, variations in  $K_{d,\lambda}$  values are less than 5% (Hargreaves, 2003), an acceptable error for the present analysis.

The extinction of the filtered water samples at 305, 313, 320 and 340 nm can be rewritten into a (Naperian) absorption unit ( $\text{m}^{-1}$ ) according to the

$$A_{\lambda} = \frac{\text{Ln}(10) \times a_{\lambda,f}}{l} = \frac{2.303 \times a_{\lambda,f}}{0.001} \quad (4)$$

where  $l = 0.01$  is the path length of used quartz cuvette (in m) and  $\text{Ln}(10) = 2.303$ . Neglecting the absorption of water itself,

$$R_{\lambda} = \frac{K_{d,\lambda}}{A_{\lambda}} \quad (5)$$

where the ratio  $R_{\lambda}$  describes the portion of the spectral attenuation not associated to the direct absorption of CDOM.  $R_{\lambda}$  depends on the diffuseness of the light field and on the ratio between attenuation by the suspended and dissolved components of the water column (Kirk, 1994; Bracchini et al., 2005a).

Attenuation coefficients at 313 nm,  $K_{d,par}$  and spectral slopes are represented in a series of maps using a Kriging interpolation method (Surfer 7.0).

### 3. Results and discussion

Solar irradiance at 305 nm was highly attenuated in the waters of Katonga Bay. The maximum measured value of the attenuation coefficient was  $50 \text{ m}^{-1}$  and minimum was  $9 \text{ m}^{-1}$ . In nine stations, the attenuation coefficient could not be calculated due to the limited penetration of this spectral irradiance. In Bunjako Bay, the maximum value of  $K_{d,305}$  was  $14 \text{ m}^{-1}$  and the minimum was  $7 \text{ m}^{-1}$ . For the other three attenuation coefficients (at 313, 320 and 340 nm), all measurements were accepted and the average values of attenuation coefficients are presented in Table 1. High values of attenuation coefficients were observed in the two bays (the first

row) with high spatial heterogeneity (SD). The average  $K_{d,\lambda}$  values as well as the spatial variation was higher in Katonga Bay in all UV wavelengths and PAR.

As the attenuation coefficients at 305, 320 and 340 nm were linearly related with attenuation coefficients at 313 nm (Fig. 2), this parameter was used to examine the spatial distribution of UV attenuation used for the geographical representation.  $K_{d,303}$  showed maximum values nearest to the river inflow in Katonga Bay and a general reduction along the bay (Fig. 3). Near the western and south western coasts, the attenuation coefficients were between 46 and  $38 \text{ m}^{-1}$  and the central part of the Katonga Bay has value around  $30 \text{ m}^{-1}$ . At 3 km from the wetland border, the attenuation coefficient values decrease to  $24 \text{ m}^{-1}$ . This demonstrates the influence of the river inflow and the release of dissolved organic (and suspended) matter on the optical properties of the bay. In these high attenuation areas, closest to the wetland, incoming solar ultraviolet radiation was

Table 1

Average optical properties and standard deviations (SD) of Katonga and Bunjako Bays, average attenuation coefficients ( $K_{d,\lambda}$ ), average  $R_z$ , average  $P_{313,f}$  and average  $P_{313,nf-f}$

	$K_{d,313} \text{ (m}^{-1}\text{)}$	$K_{d,320} \text{ (m}^{-1}\text{)}$	$K_{d,340} \text{ (m}^{-1}\text{)}$	$K_{d,par} \text{ (m}^{-1}\text{)}$	$R_{305}$	$R_{313}$	$R_{320}$	$R_{340}$	$P_{313,f}$	$P_{313,nf-f}$
All stations	16	15	13	3						
SD	12	12	9	1						
Katonga Bay	30	28	24	3	1.4	1.7	1.8	2.1	0.5	0.5
SD	11	10	8	1	0.5	0.5	0.6	0.8	0.2	0.2
Bunjako Bay	9	8	7	2.0	3	3	3	2	0.2	0.8
SD	2	2	2	0.4	2	2	2	2	0.1	0.1

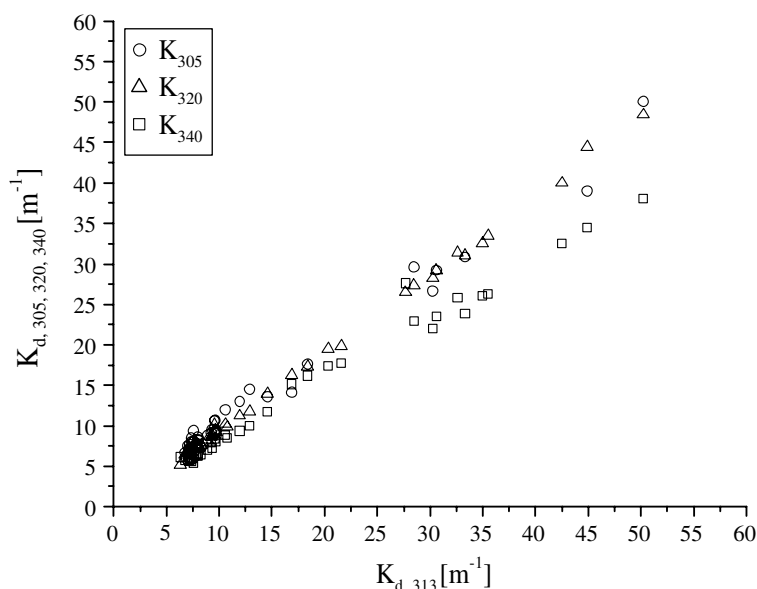


Fig. 2. UV attenuation coefficients ( $\text{m}^{-1}$ ) at 313 nm shown in comparison to attenuation coefficients at 305, 320 and 340 nm in Katonga and Bunjako Bays.

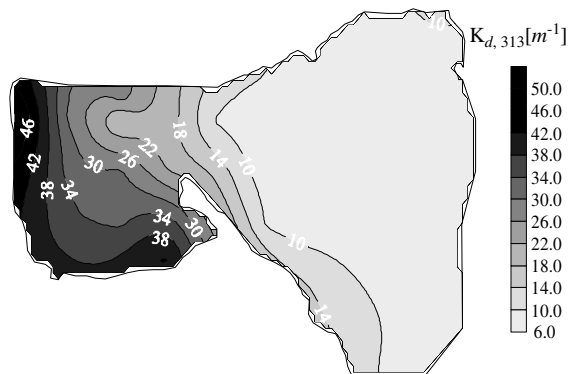


Fig. 3. Spatial distribution of the attenuation coefficients ( $\text{m}^{-1}$ ) at 313 nm in Katonga Bay and Bunjako Bay.

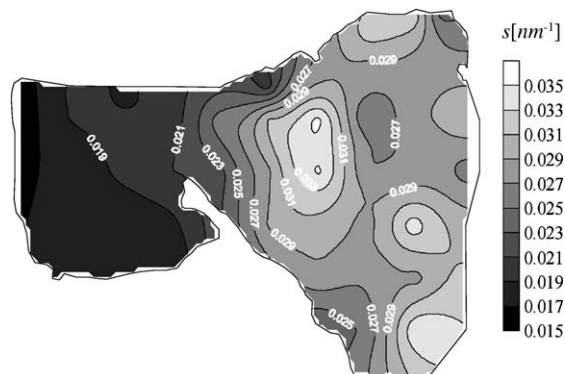


Fig. 5. Spatial distribution of the spectral slope ( $\text{nm}^{-1}$ ) of CDOM in Katonga Bay and Bunjako Bay.

strongly absorbed (and scattered) in the few centimeters of the water column. As the column depth in these stations was between 0.8 m (station 1b) and 3.0 m (station 15), a large percentage of the water column was characterized by a  $I/I_0$  ratio lower than 1% at 313 nm. In the Bunjako Bay, the  $K_{d,313}$  values were between 6 and  $18 \text{ m}^{-1}$ , with a large area between 6 and  $10 \text{ m}^{-1}$ . Lower values of  $K_{d,313}$  and a limited spatial variation differentiates Bunjako Bay with respect to Katonga Bay.

In aquatic ecosystems, the major constituent which absorb UV radiation is CDOM. Wetland released CDOM appears to strongly influence the optical properties of Katonga Bay in particular near the western and southwestern coastal line. The eastern spatial gradient could be explained by dilution and/or by a biological or solar modification of CDOM optical properties. The spatial distribution of the attenuation coefficient in the PAR band showed maximum values nearest to the river inflow ( $7.5 \text{ m}^{-1}$ ) and in south western ( $5.5 \text{ m}^{-1}$ ) part of Katonga Bay (Fig. 4). In this bay, the availability of solar

radiation for photosynthesis is controlled by both concentrations of phytoplankton as well as the wetland released organic matter.

The spatial distribution of the spectral slope (Eq. (2)) showed a high spatial variation, in particular in Bunjako Bay (Fig. 5). The lowest values were observed in Katonga Bay, at the river inlet and wetland coast ( $0.015 \text{ nm}^{-1}$ ) and the highest values were observed in the outer bay ( $0.035 \text{ nm}^{-1}$ ). This increase in the spectral slope could be explained by a number of factors: difference in the quality of the released CDOM at terrestrial sources, bacterial degradation of the organic matter or photodegradation due to the absorption of the incoming UV solar radiation (photobleaching). CDOM in the two bays clearly shows a different ability to absorb ultraviolet radiation. Even if the dissolved organic carbon concentrations in these two bays were similar (probably this is not the case), the efficiency in absorbing solar ultraviolet radiation in the Katonga Bay is greater than in Bunjako Bay (according to the spectral slope values). Further analysis should be conducted to analyze the spatial variation of a specific absorption (ratio between absorption at 375 nm and the measured dissolved organic carbon).

By correlating the spectral slope and  $A_{313,f}$  for each measurement site (Fig. 6), differences between the optical properties of the two bays is clearly shown in fact low spectral slope/high absorption values for Katonga Bay and high spectral slope/low absorption values in Bunjako Bay. Stedmon and Markager (2001, 2003) used such patterns in marine ecosystems to distinguish between terrestrial CDOM inputs and production related CDOM. In the present work, a similar interpretation can be made where terrigenous (wetland) CDOM sources dominate Katonga Bay and a mixture of degraded terrigenous and phytoplankton generated CDOM are present in Bunjako Bay. The points in the transitional zone are located between two bays.

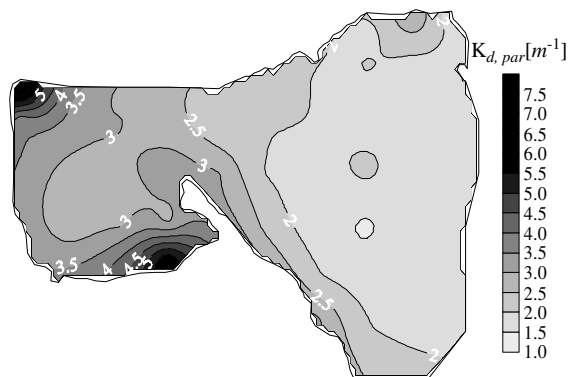


Fig. 4. PAR attenuation coefficients ( $\text{m}^{-1}$ ) in Katonga Bay and Bunjako Bay.

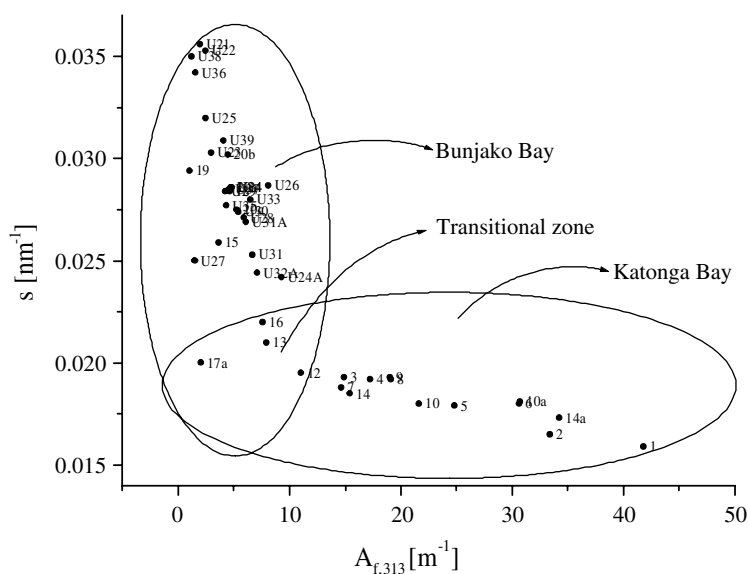


Fig. 6. Spectral slope ( $\text{nm}^{-1}$ ) values versus 313 nm Naperian extinction ( $\text{m}^{-1}$ ) values in Katonga Bay and Bunjako Bay. The horizontal ellipse represents all stations in the Katonga Bay and the vertical ellipse represents stations in Bunjako Bay. The intersection represents a transitional zone between the two bays. Labels represent station names.

$P_{\lambda,f}$  and  $P_{\lambda,nf-f}$  ratios (Eq. (3)) were determined at 313 nm to examine the relative role of suspended and dissolved matter in the overall extinction (Table 1, the last two columns). In Katonga Bay, suspended particles and CDOM played a similar role in the extinction at 313 nm ( $P_{313,f} = P_{313,nf-f} = 0.5$ ). In the Bunjako Bay, the role of suspended particles ( $P_{313,nf-f} = 0.8$ ) was greater than CDOM ( $P_{313,f} = 0.2$ ).

Linear correlations between  $K_{d,\lambda}$  and the absorbance of the filtered samples ( $a_{\lambda,f}$ ) were found: at 305 nm, the angular coefficient ( $m$ ) was  $222 \pm 12 \text{ m}^{-1}$  ( $N = 37$ ,  $R = 0.96$ ,  $p < 1 \times 10^{-4}$ ), at 313 nm;  $m = 266 \pm 14$  ( $N = 46$ ,  $R = 0.94$ ,  $p < 1 \times 10^{-4}$ ), at 320 nm;  $m = 282 \pm 16$  ( $N = 46$ ,  $R = 0.93$ ,  $p < 1 \times 10^{-4}$ ) and at 340 nm;  $m = 290 \pm 23$  ( $N = 46$ ,  $R = 0.89$ ,  $p < 1 \times 10^{-4}$ ). The correlation between AOPs ( $K_{d,\lambda}$ ) and IOPs ( $a_{\lambda,f}$ ) supports the hypothesis that changes in  $K_{d,\lambda}$  values are not related to changes in incident radiation (solar zenith angle) and variation of  $K_{d,\lambda}$  values caused by shifting of shape of solar spectra (with the solar zenith angle variation) can be neglected.

The  $R_{\lambda}$  ratio (Eq. (5)) showed higher average values and standard deviations in Bunjako Bay with respect to Katonga Bay (Table 1). In Katonga, the attenuation coefficients in the UV band were more influenced by the direct extinction by CDOM. In Bunjako Bay, suspended particles play a more important role in the attenuation of UV solar radiation. In Katonga Bay, the relatively high concentration and low slope of CDOM are responsible for its dominating role in the attenuation of poten-

tial harmful UV-B (290–320 nm) and UV-A (320–400 nm) bands of the solar radiation.

#### 4. Conclusions

Spectrophotometric analyses performed in two Ugandan Bays of Lake Victoria clearly demonstrated the importance of river and wetland connections on the optical and bio-optical properties of the lake waters. Clear differences were observed between bays, and these differences were associated with the spectral characteristics and concentration of CDOM. The inflow of large quantities of CDOM with a strong absorption in the UV wavelengths strongly influences the availability of solar radiation in Katonga Bay. UV attenuation coefficients are dominated by the absorption of CDOM and shows a clear spatial distribution within the bay. The spatial pattern of slope values measured in Katonga further support this hypothesis. A similar spatial distribution of  $K_{d,par}$  suggests that CDOM plays an important role in the attenuation of the visible radiation.

Littoral and riverine wetlands release high concentrations of CDOM which is characterized by a low spectral slope and a high capacity to absorb short wavelength solar radiation. Such conditions allow for a low penetration of harmful UV radiation. Further from the terrestrial sources, CDOM appears to be degraded and/or originated from other sources. Its ability to shield the ecosystem from fluxes of UV radiation is much lower.

The high fluxes of solar radiation in an equatorial zone such as Lake Victoria underline the fundamental importance of wetland ecosystems in modifying the optical and biological characteristics of the water column. The presence of coastal areas with a water column relatively free from the most harmful UV radiation may be fundamental for the protection of aquatic organisms such as fish larvae and amphibians.

### Acknowledgements

This research was supported through the European Commission DG RTDINCO DEV programme (ICA4-CT-2001-10036). Satellite images were obtained in collaboration with CONAE-Argentina. Researchers were supported by the Italian Interuniversity Consortium CSGI.

### References

- Akkanen, J., Lyytikäinen, M., Tuikka, A., Kukkonen, J.V.K., 2005. Dissolved organic matter in pore water of freshwater sediments: effects of separation procedure on quantity, quality and functionality. *Chemosphere* 60, 1608–1615.
- Backlund, P., 1992. Degradation of aquatic humic material by ultraviolet light. *Chemosphere* 25, 1869–1878.
- Baker, K.S., Smith, R.C., 1979. Quasi-inherent characteristics of diffuse attenuation coefficient of irradiance. *Ocean Optics VI SPIE* 208, 60–63.
- Bracchini, L., Cozar, A., Dattilo, A.M., Falcucci, M., Gonzales, R., Loiselle, S., Hull, V., 2004a. Analysis of extinction in ultraviolet and visible spectra of water bodies of the Paraguay and Brazil wetlands. *Chemosphere* 57, 1245–1255.
- Bracchini, L., Loiselle, S.A., Dattilo, A.M., Mazzuoli, S., Cózar, A., Rossi, C., 2004b. The spatial distribution of the optical properties in the UV and visible in an aquatic ecosystem. *Photochem. Photobiol.* 80, 139–149.
- Bracchini, L., Dattilo, A.M., Falcucci, M., Loiselle, S.A., Hull, V., Arena, C., Rossi, C., 2005a. Spatial and temporal variation of the inherent and apparent optical properties in a shallow coastal lake. *J. Photochem. Photobiol.* 80, 161–177.
- Bracchini, L., Cózar, A., Dattilo, A.M., Picchi, M.P., Arena, C., Mazzuoli, S., Loiselle, S., 2005b. Modelling the components of the vertical attenuation of ultraviolet radiation in a wetland lake ecosystem. *Ecol. Mod.* 186, 43–54.
- Bricaud, A., Morel, A., Prieur, L., 1981. Absorption by dissolved organic matter of the sea (yellow substance) in the UV and visible domains. *Limnol. Oceanogr.* 26, 43–53.
- Corin, N., Backlund, P., Kulovaara, M., 1996. Degradation products formed during UV-irradiation of humic waters. *Chemosphere* 33, 245–255.
- Corin, N., Backlund, P., Wiklund, T., 1998. Bacterial growth in humic waters exposed to UV-radiation and simulated sunlight. *Chemosphere* 36, 1947–1958.
- Danielson, L.G., 1982. On the use of filters for distinguishing between dissolved and particulate fractions in natural waters. *Water Res.* 16, 179–182.
- De Haan, H., 1972. Molecule-size distribution of soluble humic compounds from different natural waters. *Freshwater Biol.* 2, 235–241.
- Grzybowski, W., 2000. Effect of short-term sunlight irradiation on absorbance spectra of chromophoric organic matter dissolved in coastal and riverine water. *Chemosphere* 40, 1313–1318.
- Haag, W.R., Hoigné, J., Gassman, E., Braun, A.M., 1984. Singlet oxygen in surface waters—Part II: Quantum yields of its production by some natural humic materials as a function of wavelength. *Chemosphere* 13, 641–650.
- Hansell, D.A., Carlson, C.A., 2002. *Biogeochemistry of Marine Dissolved Organic Matter*. Academic Press, San Diego.
- Hargreaves, B.R., 2003. Water column optics and penetration of UVR. In: Helbling, E.W., Zagarese, H. (Eds.), *UV Effects in Aquatic Organisms and Ecosystems*. The Royal Society of Chemistry, Cambridge, UK, pp. 59–105.
- Hunt, A.P., Parry, J.D., Hamilton-Taylor, J., 2000. Further evidence of elemental composition as an indicator of the bioavailability of humic substances to bacteria. *Limnol. Oceanogr.* 45, 237–241.
- Huovinen, P.S., Penttilä, H., Soimasuo, M.R., 2003. Spectral attenuation of solar ultraviolet radiation in humic lakes in Central Finland. *Chemosphere* 51, 205–214.
- Kalbitz, K., Geyer, S., Geyer, W., 2000. A comparative characterization of dissolved organic matter by means of original aqueous samples and isolated humic substances. *Chemosphere* 40, 1305–1312.
- Kirk, J.T.O., 1994. *Light and Photosynthesis in Aquatic Ecosystems*. Cambridge University Press, Cambridge.
- Markager, S., Vincent, W.F., 2000. Spectral light attenuation and absorption of UV and blue light in the natural waters. *Limnol. Oceanogr.* 45, 642–650.
- McDonald, S., Bishop, A.G., Prenzler, P.D., Robards, K., 2004. Analytical chemistry of freshwater humic substances. *Anal. Chim. Acta* 527, 105–124.
- McKnight, D.M., Aiken, G.R., 1998. Aquatic humic substances: ecology and biogeochemistry. In: Hessen, D.O., Tranvik, L.J. (Eds.), *Ecological Studies*, vol. 1. Springer-Verlag, Berlin, pp. 9–39.
- Morris, D.P., Zagarese, H., Williamson, C.E., Balseiro, E.G., Hargreaves, B.R., Modenutti, B., Moeller, R., Queimalinos, C., 1995. The attenuation of solar UV radiation in lakes and the role of dissolved organic carbon. *Limnol. Oceanogr.* 40, 1381–1391.
- Osburn, C.L., Morris, D.P., 2003. Photochemistry of chromophoric dissolved organic matter in natural waters. In: Helbling, E.W., Zagarese, H. (Eds.), *UV Effects in Aquatic Organisms and Ecosystems*. The Royal Society of Chemistry, Cambridge, pp. 185–217.
- Peuravuori, J., Pihlaja, K., 1997. Molecular size distribution and spectroscopic properties of aquatic humic substances. *Anal. Chim. Acta* 337, 133–149.
- Shindler, D.W., Jefferson-Curtis, P., Parker, B.R., Stainton, M.P., 1996. Consequences of climate warming and lake acidification for UV-B penetration in North American boreal lakes. *Nature* 379, 705–708.

- Stedmon, C.A., Markager, S., 2001. The optics of chromophoric dissolved organic matter (CDOM) in the Greenland Sea: an algorithm for differentiation between marine and terrestrial derived organic matter. *Limnol. Oceanogr.* 46, 2087–2093.
- Stedmon, C.A., Markager, S., 2003. Behaviour of the optical properties of coloured dissolved organic matter under conservative mixing. *Estuar. Coast. Shelf S.* 57, 973–979.
- Stedmon, C.A., Markager, S., Kaas, H., 2000. Optical properties and signature of chromophoric dissolved organic matter (CDOM) in Danish coastal waters. *Estuar. Coast. Shelf S.* 51, 267–278.
- Vincent, W.F., Rae, R., Laurion, I., Howard-Williams, C., Priscu, J.C., 1998. Transparency of Antarctic ice-covered lakes to solar UV radiation. *Limnol. Oceanogr.* 43, 618–624.
- Williamson, C.E., Morris, D.P., Pace, M.L., Olson, O.G., 1999. Dissolved organic carbon and nutrients as regulators of lake ecosystems: resurrection of a more integrated paradigm. *Limnol. Oceanogr.* 44, 795–803.
- Zafriou, O.C., 2002. Sunburnt organic matter: biogeochemistry of light-altered substrate. *Limnol. Oceanogr. Bull.* 11, 69–74.
- Zanardi-Lamardo, E., Moore, C.A., Zika, R.G., 2004. Seasonal variation in molecular mass and optical properties of chromophoric dissolved organic matter in coastal waters of southwest Florida. *Mar. Chem.* 89, 37–54.
- Zepp, R.G., 2003. Solar UVR and aquatic carbon, nitrogen, sulphur and metal cycles. In: Helbling, E.W., Zagarese, H. (Eds.), *UV Effects in Aquatic Organisms and Ecosystems*. The Royal Society of Chemistry, Cambridge, pp. 137–183.
- Zepp, R.G., Callaghan, T.V., Erickson III, D.J., 2003. Interactive effects of ozone depletion and climate change on biogeochemical cycles. *Photochem. Photobiol. Sci.* 2, 51–61.
- Zheng, X., Dickey, T., Chang, G., 2002. Variability of the downwelling diffuse attenuation coefficient with consideration of inelastic scattering. *Appl. Opt.* 41, 6477–6488.